Psychiatry Research: Neuroimaging 336 (2023) 111735

Contents lists available at ScienceDirect

Psychiatry Research: Neuroimaging

journal homepage: www.elsevier.com/locate/psychresns

Short communication

Standardizing MRI orientation improves reliability of entorhinal and transentorhinal cortical volume measurement

Yi-En Quek [a,*], Yi Leng Fung [a], Simon J. Vogrin [b], Pierrick Bourgeat [c], Sara Vogrin [d], Jurgen Fripp [c], Steven J. Collins [b,e], Stephen C. Bowden [a,b], for the Alzheimer's Disease Neuroimaging Initiative#

[a] Melbourne School of Psychological Sciences, The University of Melbourne, Parkville, Victoria, Australia
[b] Department of Clinical Neurosciences, St Vincent's Hospital Melbourne, Fitzroy, Victoria, Australia
[c] The Australian e-Health Research Centre, CSIRO Health and Biosecurity, Herston, Queensland, Australia
[d] Department of Medicine, St Vincent's Hospital Melbourne, The University of Melbourne, Fitzroy, Victoria, Australia
[e] Department of Medicine, The Royal Melbourne Hospital, The University of Melbourne, Parkville, Victoria, Australia

ARTICLE INFO

Keywords:
Magnetic resonance imaging
Entorhinal cortex
Transentorhinal cortex

ABSTRACT

The current study compared the reliability of manual collateral sulcus depth and entorhinal and transentorhinal cortical volume measurements between native oriented MRI scans versus MRI scans realigned to the hippocampal long axis. Data included 10 participants with two serial 3.0T MRI scans from the Alzheimer's Disease Neuroimaging Initiative. Both collateral sulcus depth and entorhinal and transentorhinal cortical volume measurement reliability improved from the native to the hippocampal oriented scans. Standardizing scan orientation is important to optimize reliability of MRI-derived manual measurements of the entorhinal and transentorhinal cortices. In quantitative MRI studies, aligning scans to a common, normalized orientation is recommended.

1. Introduction

Volume measurements of the entorhinal and transentorhinal cortices may provide valuable early markers of Alzheimer's disease (AD) as these regions are among the earliest in the brain to show clinically correlated structural changes (Kulason et al., 2019; Kulason et al., 2020). Recent guidelines for the measurement of the entorhinal and transentorhinal cortices on magnetic resonance imaging (MRI) scans have incorporated anatomical variations of the depth of the collateral sulcus to provide more precise segmentation rules for the entorhinal and transentorhinal cortices (Berron et al., 2017; Kivisaari et al., 2013; Yushkevich et al., 2015). However, in measuring collateral sulcus depth and entorhinal and transentorhinal cortical volumes, it is important to consider extraneous variables that may introduce variability in these measurements. One such variable is MRI scan orientation (Plante and Turkstra, 1991). Whilst scan orientation is generally standardized during acquisition, some variation across patients is unavoidable. These variations can result in substantial variations in MRI-derived manual measurements (Bartzokis et al., 1998; Hasboun et al., 1996). Nonetheless, many studies employing MRI-derived manual measurements either do not reorient scans to a normalized orientation or do not report doing so (Geuze et al., 2005). The current study aimed to compare the reliability of manual collateral sulcal depth measurements and entorhinal and transentorhinal cortical volume measurements between native oriented MRI scans versus MRI scans realigned to a common, normalized orientation.

2. Methods

2.1. Neuroimaging data

The sample included 10 participants with two serial 3.0T MRI scans within a 3-month interval from the Alzheimer's Disease Neuroimaging Initiative (ADNI) database. Although head positioning at each MRI examination in ADNI is standardized by aligning the centering crosshairs

* Corresponding author at: Melbourne School of Psychological Sciences, Redmond Barry Building, The University of Melbourne, Parkville, VIC 3010, Australia.
E-mail address: yien@student.unimelb.edu.au (Y.-E. Quek).

Data used in preparation of this article were obtained from the Alzheimer's Disease Neuroimaging Initiative (ADNI) database (adni.loni.usc.edu). As such, the investigators within the ADNI contributed to the design and implementation of ADNI and/or provided data but did not participate in analysis or writing of this report. A complete listing of ADNI investigators can be found at: http://adni.loni.usc.edu/wp-content/uploads/how_to_apply/ADNI_Acknowledgement_List.pdf

https://doi.org/10.1016/j.pscychresns.2023.111735
Received 3 June 2023; Received in revised form 14 September 2023; Accepted 9 October 2023
Available online 18 October 2023

on the participant's nasion, slight variations in head positioning still occur across the ADNI dataset. Hence, the serial scans were selected to highlight the inherent variation in head positioning between the two acquisitions. To select the scans, the ADNI baseline and 3- and 6-month follow-up scans were first ranked according to the difference in head position angle between the serial scans. Further description of the determination of the difference in head position angle is presented in the Supplementary Material. From the 50 pairs of serial scans with the largest difference in head position angle, 10 pairs of serial scans (either the baseline and 3-month follow-up scans or the 3-month and 6-month follow-up scans) were randomly selected. The initial scan was denoted as Time 1, and the subsequent 3-month scan was denoted as Time 2. At Time 1, the 10 selected MRI scans comprised two healthy controls, six participants with amnestic mild cognitive impairment (aMCI), and two participants with AD dementia (age range = 56–78 years).

2.2. Data preprocessing

The raw DICOM images were converted to NIfTI format and processed using FreeSurfer v6.0 (Sánchez–Benavides et al., 2010). The MRI scans were then resampled to $0.3 \times 0.3 \times 1.0$ mm^3 (original resolution $= 1.0 \times 1.0 \times 1.2$ mm^3) by cubic spline interpolation to improve in-plane image resolution for estimating structural boundaries. The hippocampal long axis was chosen as the reference angle for reorientation of the scans as it is easy to identify and is widely used to visualize the mesial temporal structures (Geuze et al., 2005). A python script using the SimpleITK library (v.2.1.0rc1.post39) was created to reorient the resampled scans to the hippocampal long axis on the sagittal plane (https://doi.org/10.25919/8kjn-d006). The operation of the python script is summarized in the Supplementary Material.

2.3. Manual segmentation

Manual segmentation was conducted using ITK-SNAP Version 3.8.0 (Yushkevich et al., 2006). The entorhinal and transentorhinal cortices were segmented according to the Berron et al. (2017) segmentation protocol. Collateral sulcus depth was measured during the entorhinal and transentorhinal segmentation procedure and was categorized into the six collateral sulcus depth types outlined in the Berron et al. (2017) segmentation protocol to use in subsequent statistical analyses.

A single rater blind to participants' diagnosis completed all manual segmentations. Manual segmentations on 10 randomly selected MRI scans (evenly split between the native and hippocampal oriented scans and between the Time 1 and Time 2 scans) were repeated to assess intra-rater reliability and conducted by an independent rater to assess inter-rater reliability. The order of segmentation of the native and hippocampal oriented scans were randomized.

2.4. Statistical analysis

Intra- and inter-rater reliability of the collateral sulcus depth types were evaluated using the linear and quadratic weighted kappa (κ_{linear} and $\kappa_{quadratic}$) statistics. Intra- and inter-rater reliability of the entorhinal cortex and transentorhinal cortex volume measurements were evaluated using the intraclass correlation coefficient (ICC) statistic.

Reliability of the collateral sulcus depth types between Time 1 and Time 2 on the native and hippocampal oriented scans was evaluated using the κ_{linear} and $\kappa_{quadratic}$ statistics. Reliability of the entorhinal cortex and transentorhinal cortex volume measurements between Time 1 and Time 2 on the native and hippocampal oriented scans was evaluated using the ICC statistic and the Bland–Altman method (Altman and Bland, 1983; Bland and Altman, 1986). For each serial volume measurement, the percentage change in volume was plotted against the mean volume.

3. Results

3.1. Intra- and inter-rater reliability

For the collateral sulcus depth types, intra-rater reliability was $\kappa_{linear} = 0.98$ (95% CI 0.97–0.99) and $\kappa_{quadratic} = 0.99$ (95% CI 0.99–0.99), and inter-rater reliability was $\kappa_{linear} = 0.72$ (95% CI 0.68–0.76) and $\kappa_{quadratic} = 0.86$ (95% CI 0.83–0.89).

For the entorhinal cortex volume measurements, intra-rater reliability was ICC = 0.89 (95% CI 0.54–0.96), and inter-rater reliability was ICC = 0.93 (95% CI 0.91–0.99). For the transentorhinal cortex volume measurements, intra-rater reliability was ICC = 0.87 (95% CI 0.43–0.96), and inter-rater reliability was ICC = 0.72 (95% CI 0.42–0.88).

3.2. Reliability of collateral sulcus depth types

There were $n = 503$ and $n = 538$ MRI slices (10 participants $\times$ 2 hemispheres) that contained a measured collateral sulcus on the native and hippocampal oriented scans, respectively. The reliability of the collateral sulcus depth types between Time 1 and Time 2 on the native oriented scans was $\kappa_{linear} = 0.71$ (95% CI 0.67–0.76) and $\kappa_{quadratic} = 0.80$ (95% CI 0.75–0.85) but significantly improved on the hippocampal oriented scans to $\kappa_{linear} = 0.87$ (95% CI 0.84–0.90) and $\kappa_{quadratic} = 0.92$ (95% CI 0.90–0.95). Table S1 presents the cross-tabulation matrix of the collateral sulcus depth types between Time 1 and Time 2 on the native and hippocampal oriented scans.

3.3. Reliability of entorhinal cortex and transentorhinal cortex volume measurements

For the entorhinal cortex, the reliability of the volume measurements between Time 1 and Time 2 on the native oriented scans was ICC = 0.67 (95% CI 0.33–0.86) but significantly improved on the hippocampal oriented scans to ICC = 0.90 (95% CI 0.77–0.96). For the transentorhinal cortex, the reliability of the volume measurements between Time 1 and Time 2 on the native oriented scans was ICC = 0.62 (95% CI 0.27–0.83) but also significantly improved on the hippocampal oriented scans to ICC = 0.94 (95% CI 0.85–0.98).

Fig. 1 presents Bland–Altman plots showing the percentage change in entorhinal and transentorhinal volumes between Time 1 and Time 2 on the native and hippocampal oriented scans. For the entorhinal cortex, the variability in volumes, as indicated by the 95% agreement limits and corresponding 95% CIs, on the hippocampal oriented scans was considerably less than on the native oriented scans. For the transentorhinal cortex, the same trend was observed, with reduced variability in volumes on the hippocampal oriented scans relative to the native oriented scans.

4. Discussion

The results of the current study showed consistently higher reliability estimates for both manual collateral sulcus depth as well as entorhinal and transentorhinal cortical volume measurements for scans aligned to a common, normalized orientation compared to native oriented scans. These results suggest that aligning MRI scans to a common orientation improves the reliability of manually obtained MRI measurements. The findings of the current study are in line with a previous study that observed less variability in amygdala, hippocampal, and temporal lobe volumes in scans aligned to a common orientation compared to scans not aligned to a common orientation (Bartzokis et al., 1998). Variations in head positioning during MRI acquisition can lead to variations in how brain structures are visualized on the MR images (Plante and Turkstra, 1991; Reuter et al., 2014). Variations in how the entorhinal and transentorhinal cortices are visualized could result in substantial variability in subsequent volume measurements depending

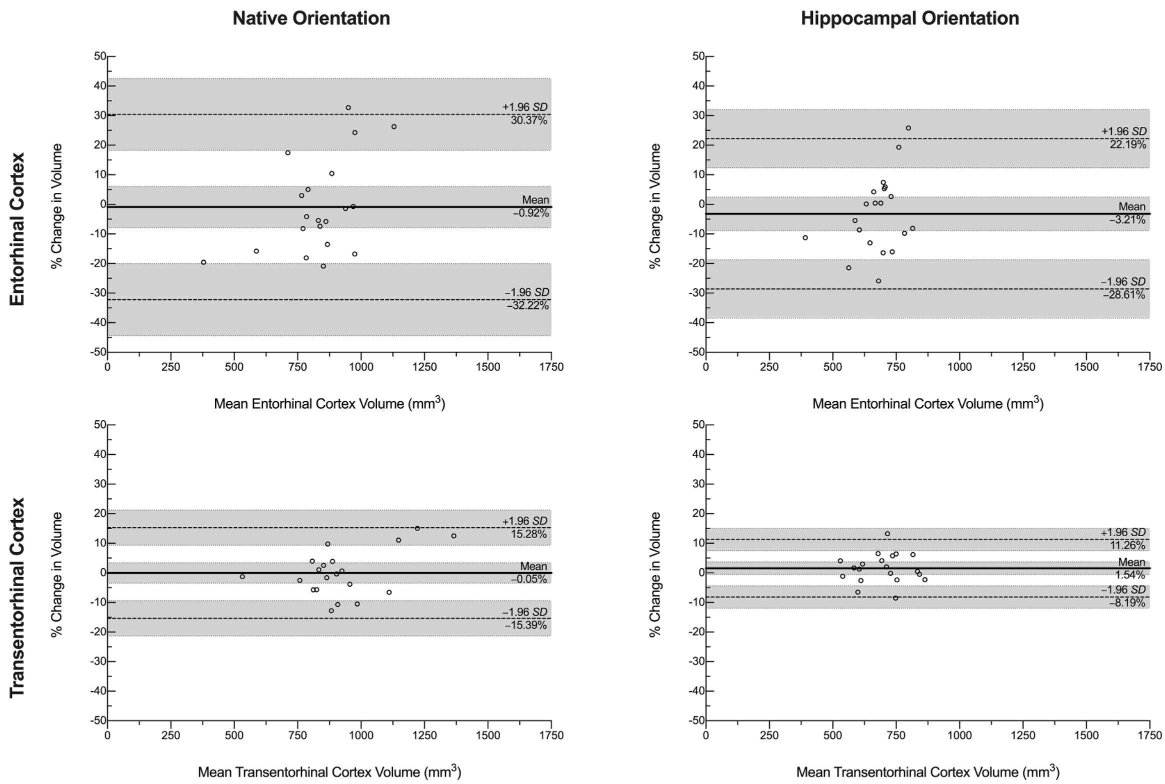

Fig. 1. Bland–Altman plots showing percentage change in volume against mean volume between Time 1 and Time 2 on the native and hippocampal oriented MRI scans.
Note. Solid lines represent mean percentage change in volume between Time 1 and Time 2. Dashed lines represent 95% agreement limits and shaded areas represent corresponding 95% CIs.

on how much structure is visible.

One limitation of the current study is that the 3-month interval between MRI scans may have introduced extraneous variables that alter brain morphology and thus impacted the depth and volume measurements (Duning et al., 2005; Hagemann et al., 2011). Nevertheless, because the scans in the common orientation condition were the same scans as in the native orientation condition except realigned, any impact on the depth and volume measurements due to extraneous variables should be present in both conditions. Therefore, the observed improvement in reliability of the depth and volume measurements may be concluded to be attributable to the standardization in orientation.

The results of the current study highlight the importance of aligning MRI scans to a common orientation to obtain reliable volume measurements of structures of interest. Notably, there has been growing interest in automated brain volumetric segmentation tools, which typically rely on manually segmented scans as training data (Singh and Singh, 2021). For these tools to provide reliable measurements, it is essential that the procedures used to obtain the manual segmentation training data optimize reliability. Standardizing MRI scan orientation is a simple step toward improving the reliability of manual segmentations.

Declaration of Competing Interest

The authors declare that they have no known competing financial interests or personal relationships that could have appeared to influence the work reported in this paper.

Acknowledgement

This work was supported by the Australian Commonwealth Government and the University of Melbourne.

Data used in the preparation of this article were obtained from the Alzheimer's Disease Neuroimaging Initiative (ADNI) database (adni.loni.usc.edu). The ADNI was launched in 2003 as a public-private partnership, led by Principal Investigator Michael W. Weiner, MD. The primary goal of ADNI has been to test whether serial magnetic resonance imaging (MRI), positron emission tomography (PET), other biological markers, and clinical and neuropsychological assessment can be combined to measure the progression of mild cognitive impairment (MCI) and early Alzheimer's disease (AD). For up-to-date information, see www.adni-info.org.

Data collection and sharing for this project was funded by the Alzheimer's Disease Neuroimaging Initiative (ADNI) (National Institutes of Health Grant U01 AG024904) and DOD ADNI (Department of Defense award number W81XWH-12-2-0012). ADNI is funded by the National Institute on Aging, the National Institute of Biomedical Imaging and Bioengineering, and through generous contributions from the following: AbbVie, Alzheimer's Association; Alzheimer's Drug Discovery Foundation; Araclon Biotech; BioClinica, Inc.; Biogen; Bristol-Myers Squibb Company; CereSpir, Inc.; Cogstate; Eisai Inc.; Elan Pharmaceuticals, Inc.; Eli Lilly and Company; EuroImmun; F. Hoffmann-La Roche Ltd and its affiliated company Genentech, Inc.; Fujirebio; GE Healthcare; IXICO Ltd.;Janssen Alzheimer Immunotherapy Research & Development, LLC.; Johnson & Johnson Pharmaceutical Research & Development LLC.; Lumosity; Lundbeck; Merck & Co., Inc.;Meso Scale Diagnostics, LLC.; NeuroRx Research; Neurotrack Technologies; Novartis Pharmaceuticals Corporation; Pfizer Inc.; Piramal Imaging; Servier; Takeda Pharmaceutical Company; and Transition Therapeutics. The Canadian Institutes of Health Research is providing funds to support ADNI clinical sites in Canada. Private sector contributions are facilitated by the Foundation for the National Institutes of Health (www.fnih.org). The grantee organization is the Northern California Institute for Research and Education, and the study is coordinated by the Alzheimer's Therapeutic Research Institute at the University of Southern California. ADNI data are

disseminated by the Laboratory for Neuro Imaging at the University of Southern California.

Supplementary materials

Supplementary material associated with this article can be found, in the online version, at doi:10.1016/j.pscychresns.2023.111735.

References

Altman, D.G., Bland, J.M., 1983. Measurement in medicine: the analysis of method comparison studies. J. Royal Stat. Soc. Series D (The Statistician) 32, 307–317.
Bartzokis, G., Altshuler, L.L., Greider, T., Curran, J., Keen, B., Dixon, W., 1998. Reliability of medial temporal lobe volume measurements using reformatted 3D images. Psychiatry Res. Neuroimag. 82, 11–24.
Berron, D., Vieweg, P., Hochkeppler, A., Pluta, J.B., Ding, S.-L., Maass, A., Luther, A., Xie, L., Das, S.R., Wolk, D.A., Wolbers, T., Yushkevich, P.A., Düzel, E., Wisse, L.E.M., 2017. A protocol for manual segmentation of medial temporal lobe subregions in 7 Tesla MRI. NeuroImage Clin. 15, 466–482.
Bland, J.M., Altman, D.G., 1986. Statistical methods for assessing agreement between two methods of clinical measurement. Lancet 327, 307–310.
Duning, T., Kloska, S., Steinsträter, O., Kugel, H., Heindel, W., Knecht, S., 2005. Dehydration confounds the assessment of brain atrophy. Neurology 64, 548–550.
Geuze, E., Vermetten, E., Bremner, J.D., 2005. MR-based in vivo hippocampal volumetrics: 1. Review of methodologies currently employed. Mol. Psychiatry 10, 147–159.
Hagemann, G., Ugur, T., Schleussner, E., Mentzel, H.-J., Fitzek, C., Witte, O.W., Gaser, C., 2011. Changes in brain size during the menstrual cycle. PLoS One 6, e14655.
Hasboun, D., Chantôme, M., Zouaoui, A., Sahel, M., Deladoeuille, M., Sourour, N., Duyme, M., Baulac, M., Marsault, C., Dormont, D., 1996. MR determination of hippocampal volume: comparison of three methods. Am. J. Neuroradiol. 17, 1091–1098.
Kivisaari, S.L., Probst, A., Taylor, K.I., 2013. The perirhinal, entorhinal, and parahippocampal cortices and hippocampus: An overview of functional anatomy and protocol for their segmentation in MR images. In: Ulmer, S., Jansen, O. (Eds.), The perirhinal, entorhinal, and parahippocampal cortices and hippocampus: An overview of functional anatomy and protocol for their segmentation in MR images. fMRI: Basics and Clinical Applications 239–267.
Kulason, S., Tward, D.J., Brown, T., Sicat, C.S., Liu, C.-F., Ratnanather, J.T., Younes, L., Bakker, A., Gallagher, M., Albert, M., 2019. Cortical thickness atrophy in the transentorhinal cortex in mild cognitive impairment. NeuroImage Clin. 21.
Kulason, S., Xu, E., Tward, D.J., Bakker, A., Albert, M., Younes, L., Miller, M.I., 2020. Entorhinal and transentorhinal atrophy in preclinical Alzheimer's disease. Front. Neurosci. 14.
Plante, E., Turkstra, L., 1991. Sources of error in the quantitative analysis of MRI scans. Magn. Reson. Imag. 9, 589–595.
Reuter, M., Gerstner, E.R., Rapalino, O., Batchelor, T.T., Rosen, B., Fischl, B., 2014. Impact of MRI head placement on glioma response assessment. J. Neurooncol. 118, 123–129.
Sánchez-Benavides, G., Gómez-Ansón, B., Sainz, A., Vives, Y., Delfino, M., Peña-Casanova, J., 2010. Manual validation of FreeSurfer's automated hippocampal segmentation in normal aging, mild cognitive impairment, and Alzheimer Disease subjects. Psychiatry Res. Neuroimag. 181, 219–225.
Singh, M.K., Singh, K.K., 2021. A review of publicly available automatic brain segmentation methodologies, machine learning models, recent advancements, and their comparison. Ann. Neurosci. 28, 82–93.
Yushkevich, P.A., Piven, J., Hazlett, H.C., Smith, R.G., Ho, S., Gee, J.C., Gerig, G., 2006. User-guided 3D active contour segmentation of anatomical structures: Significantly improved efficiency and reliability. NeuroImage 31, 1116–1128.
Yushkevich, P.A., Pluta, J.B., Wang, H., Xie, L., Ding, S.L., Gertje, E.C., Mancuso, L., Kliot, D., Das, S.R., Wolk, D.A., 2015. Automated volumetry and regional thickness analysis of hippocampal subfields and medial temporal cortical structures in mild cognitive impairment. Hum. Brain Mapp. 36, 258–287.